Title
Multi-Agent Cooperative Pursuit-Defense Strategy Against One Single Attacker

Journal
IEEE Robotics and Automation Letters, 5(4)

ISSN
2377-3766

Authors
Deng, Ziquan
Kong, Zhaodan

Publication Date
2020

DOI
10.1109/lra.2020.3010740

Peer reviewed

Multi-Agent Cooperative Pursuit-Defense Strategy Against One Single Attacker

Ziquan Deng and Zhaodan Kong

***Abstract*—Multiple-player games involving cooperative and adversarial agents are a type of problems of great practical significance. In this letter, we consider an attack-defense game with a single attacker and multiple defenders. The attacker attempts to enter a protected region, while the defenders attempt to defend the same region and capture the attacker outside the region. We propose a distributed pursuit-defense strategy for the defenders' cooperative defense against the attacker. Inside a bounded, convex, two-dimensional space, the defenders choose among an area-decreasing, a distance-decreasing, or a pursuing strategy. We prove that our strategy guarantees the attacker to be captured before entering the protected region in a finite time. We also demonstrate with simulations that a human-controlled attacker is unable to enter a protected region when multiple defenders are using our pursuit-defense strategy.**

***Index Terms*—Pursuit-evasion games, adversarial games, distributed robot systems, multi-robot systems.**

I. Introduction

In this letter, we propose a defense strategy for multiple defenders to defend a protected region from an attacker and capture it outside the region. Depending on the location of the attacker, our strategy assigns one of the defenders to the role of an area-decreasing defender or a distance-decreasing defender and assigns the other defenders to the roles of pursuers which take the strategy proposed in [1]. Knowing the attacker's and their neighbors' locations, the defenders can cooperatively solve the aforementioned pursuit-defense problem without knowing the attacker's strategy.

A. Related Work

The attack-defense problem in our letter is a variant of the pursuit-evasion game [1]–[4], which is a sub-class of the reach-avoid game [5]–[9]. As described in [5], a reach-avoid game is one in which an agent attempts to reach the goal region while avoiding the adversarial circumstance induced by an opposing agent. Such adversarial games are popular due to their significance in applications, such as security, fighting wildfires, and military [10].

Manuscript received March 4, 2020; accepted July 8, 2020. Date of publication July 21, 2020; date of current version July 29, 2020. This letter was recommended for publication by Associate Editor S. Berman and Editor N. Y. Chong upon evaluation of the reviewers' comments. This work was supported by the Office of Naval Research under Grant N00014-20-1-2268. *(Corresponding author: Zhaodan Kong.)*

The authors are with the Department of Mechanical and Aerospace Engineering, University of California, Davis, CA 95616 USA (e-mail: ziqdeng@ucdavis.edu; zdkong@ucdavis.edu).

Digital Object Identifier 10.1109/LRA.2020.3010740

One common approach to solve reach-avoid games is through the Hamilton-Jacobi-Isaacs (HJI) partial differential equation [11] or its numerical approximations [12], [13]. For instance, one scenario is to solve a two-player game with a HJI-based technique [14]. However, in multi-agent games, such as [6]–[9], the computation involved can be quite extensive. Chen *et al.* [6] proposed an approximate path defense solution, which is one magnitude faster than the classical HJI approach. The approximate solution was extended in [7] to take cooperation into consideration by computing maximum matching. Later a graph theoretic maximum matching approach [8] was proposed by the same group to merge pairwise outcomes for the solution of multi-player games. Built upon modified fast-marching methods (FMM), an efficient path planning algorithm was proposed in [9].

This letter focuses on the pursuit-evasion game, a sub-class of the reach-avoid game. In recent years, many efforts have been put into solving the multi-player pursuit-evasion game [15]–[18]. In the context of the single-pursuer-multiple-evader pursuit-evasion game, where the pursuer is faster than the evaders, Liu *et al.* proposed solutions based on an open-loop approach [15] and a gradient-based method [16], respectively. To incorporate a more realistic setting, where a pursuer is with uncertain position and evaders are with limited turning rates, an extended approach of the open-loop formulation was proposed in [17]. Fisac *et al.* [18] studied dynamic multi-player games through time-varying dynamics with the presence of possibly moving obstacles. Abdelkader *et al* [19] and Liang *et al.* [20] solved a three-player pursuit-evasion game where the defender aims to protect a target and capture the attacker, the goal of which is to capture the target. Efficient solutions based on model predictive control (MPC) [21], [22] and distributed algorithms [19] have also been proposed in recent years.

B. Contributions

Our work makes two major contributions. First, we enrich existing pursuit-evasion games with an additional requirement of defending a protected region (e.g., in firefighting scenarios, a group of robots must not only eliminate the fire/attacker but also protect a key infrastructure/region). Second, we propose a collaborative pursuit-defense strategy, theoretically prove its performance under mild assumptions, and demonstrate its performance in simulations where the attacker is controlled by a human.

II. Problem Formulation

Our multi-player attack-defense game is played inside a bounded, convex polygon $D \subset \mathbb{R}^2$ with a circular protected region $E \subset D$ with its center denoted by O. The game features N defenders $d^i, i = 1, \ldots, N$ and an attacker a with their dynamics defined as follows:

$$\dot{x}_a = u_a, x_a(0) = (x_a)_0, \dot{x}_{d^i} = u_{d^i}, x_{d^i}(0) = (x_{d^i})_0, \quad (1)$$

where $x_{d^i}((x_{d^i})_0) \in D$ is the (initial) position of the defender d^i, $x_a((x_a)_0) \in D$ is the (initial) position of the attacker a, and u_{d^i} and u_a are the velocity control inputs of the defender d^i and the attacker a, respectively. Assume $\|u_a(t)\|$[1]$\leq \nu_{\max}, \|u_{d^i}(t)\| \leq \nu_{\max}, \forall t \geq 0, \forall i = 1, \ldots, N$, where $\nu_{\max}$ is the maximum control input.

At any given time t, the distance between the attacker a and the group of defenders $\{d^i\}_{i=1}^N$ is defined as:

$$d_{\min}(t) = \min_{i=1,\ldots,N} \|x_{d^i}(t) - x_a(t)\| . \quad (2)$$

Then the capture condition is defined as:

$$d_{\min}(T) \leq r_c, \quad (3)$$

where $r_c > 0$ is a user-specified capture radius and $T < \infty$ is the capture time. After properly re-scaling Eqn. (1), the polytope D, and the region E, we assume $r_c = 1$ and $\nu_{\max} = 1$ in this letter.

To prevent the attacker a from entering the protected region E, the defenders $\{d^i\}_{i=1}^N$ must keep the joint configuration $\mathbf{x} := (x_a, x_{d^1}, \ldots, x_{d^N})$ within the following set:

$$\begin{aligned} D_d^* := \; &\{(\exists i, \forall x \in E, \|x_{d^i} - x\| \leq \|x_a - x\|) \\ &\cap (\forall i, \|x_{d^i} - x_a\| \geq r_c)\}, \end{aligned} \quad (4)$$

meaning that, with respect to any point of the protect region, there always exists a defender that is closer to that point than the attacker; at the same time, the distance between the attacker and any of the defenders is greater or equal to r_c.

Problem 1: (Attack-Defense Game): For any initial configuration $\mathbf{x}_0 := ((x_a)_0, (x_{d^1})_0, \ldots, (x_{d^N})_0) \in D_d^*$ and for any admissible attacker input $u_a(t)$, find a defense strategy $u_{d^i}(t)$ for each defender d^i such that i) the capture condition (Eqn. (2)) is satisfied with a finite $T < \infty$ and ii) for any $t \in (0, T]$, the trajectories defined by Eqn. (1) satisfy $\mathbf{x}(t) := (x_a(t), x_{d^1}(t), \ldots, x_{d^N}(t)) \in D_d^*$.

III. Pursuit-Defense Strategy

The basic ideas of our proposed pursuit-defense strategy are as follows. We assign a defender to implement either an *area-decreasing defense strategy* (to be presented in Section III-A) and a *distance-decreasing defense strategy* (to be presented in Section III-B). The goal of this defender is to prevent the Voronoi cell of the attacker from intersecting the protected region E. Other defenders serve as pursuers and adopt the *pursuit strategy* introduced in [1] to capture the attacker by minimizing its Voronoi cell. Our overall strategy is summarized in Algo. (1) (to be presented in Section III-C).

[1] In this letter, we use $\|.\|$ to denote the Euclidean norm $\|.\|_2$.

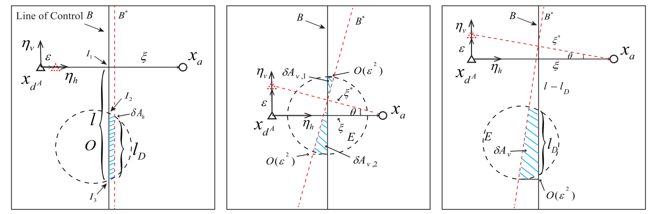

(a) (b) (c)

Fig. 1. The variational changes of A with respect to (a) a perturbation along $\boldsymbol{\eta}_h$, (b)–(c) a perturbation along $\boldsymbol{\eta}_v$ in two different cases.

In this letter, we use notations that are consistent with those of existing literature [1]–[4]. Let $V(D) = \{V_a, V_{d^i}\}$ be the Voronoi partition of D generated by the set of points $\mathbf{x} := (x_a, x_{d_1}, \ldots, x_{d_{N_D}})$, V_a be the attacker's Voronoi cell,

$$V_a = \{x \in D : \|x - x_a\| < \|x - x_{d^i}\|, \forall i \leq N\}, \quad (5)$$

V_{d^i} be the defender d^i's Voronoi cell,

$$\begin{aligned} V_{d^i} = \; &\{x \in D : \|x - x_{d^i}\| \leq \min\{\|x - x_a\|, \\ &\|x - x_{d^j}\|\}, \forall j \neq i, j \leq N\}, \end{aligned} \quad (6)$$

B_i (called a line of control [4]) be the edge shared by V_a and V_{d^i}, and L_i be the length of B_i. To be simplified, we use B to represent B_i in the later sections.

A. Area-Decreasing Defense Strategy

Let A be the intersection between the protected region E and the attacker's Voronoi cell V_a (Eqn. (5)). The attacker a can enter the region E if the intersection A is non-empty and r_c is smaller than the distance from the attacker a to the boundary of the intersection A. The time derivative of A is

$$\frac{\mathrm{d}A}{\mathrm{d}t} = \frac{\partial A}{\partial x_a}\dot{x}_a + \frac{\partial A}{\partial x_d}\dot{x}_d. \quad (7)$$

We assign a defender the role of the *area-decreasing defender* d^A by following two simple steps: i) find all defenders the Voronoi cells of which V_{d^i} (Eqn. (6)) intersect E; ii) among all such defenders, pick the one that is closest to the attacker a as d^A.

The role of the area-decreasing defender d^A is to minimize Eqn. (7). Therefore, its strategy should be

$$u_{d^A}^* \triangleq -\frac{\partial A}{\partial x_{d^A}} \Big/ \left\| \frac{\partial A}{\partial x_{d^A}} \right\|, \quad (8)$$

where we have used the assumption $\nu_{\max} = 1$.

We denote the location of the defender d^A by x_{d^A}. Then we can define a local coordinate system as shown in Fig. 1(a): let $\boldsymbol{\xi}(x_a, x_{d^A}) = x_a - x_{d^A}$ be the displacement vector pointing from the defender d^A to the attacker a; let $\boldsymbol{\eta}_h = \boldsymbol{\xi}/\|\boldsymbol{\xi}\|$; define a unit vector $\boldsymbol{\eta}_v$ that is orthogonal to $\boldsymbol{\eta}_h$ as well as pointing away from the center O of the region E; finally, the local coordinate system is specified by the two vectors $\{\boldsymbol{\eta}_h, \boldsymbol{\eta}_v\}$.

For any $y \in \mathbb{R}^2$, define

$$A^*(y) = A(x_a, y + x_{d^A}, x_{d^1}, \ldots, x_{d^{N-1}}). \quad (9)$$

Then define D_hA and D_vA as the directional derivatives of A along $\boldsymbol{\eta}_h$ and $\boldsymbol{\eta}_v$ as follows:

$$\begin{aligned} D_hA|_{\mathbf{x}} &= \lim_{\epsilon\to 0}(A^*(\epsilon\cdot\boldsymbol{\eta}_h^i)|_{\mathbf{x}} - A|_{\mathbf{x}})/\epsilon, \\ D_vA|_{\mathbf{x}} &= \lim_{\epsilon\to 0}(A^*(\epsilon\cdot\boldsymbol{\eta}_v^i)|_{\mathbf{x}} - A|_{\mathbf{x}})/\epsilon, \end{aligned} \tag{10}$$

where $\mathbf{x} := (x_a, x_{d^1}, \ldots, x_{d^{N_D}})$. Then we have the partial derivative of A with respect to x_{d^A} as follows:

$$\frac{\partial A}{\partial x_{d^A}} = D_hA\cdot\boldsymbol{\eta}_h + D_vA\cdot\boldsymbol{\eta}_v. \tag{11}$$

Lemma 1: For the area-decreasing defender d^A, it is true that

$$D_hA = -\frac{l_D}{2}, D_vA = \frac{2ll_D - l_D^2}{2\,\|\boldsymbol{\xi}\|}. \tag{12}$$

Although Eqn. (12) has the same form as the result in [4], the definitions of l and l_D are different. As shown in Fig. 1(a), point I_1 is the intersection point of $\boldsymbol{\xi}$ and the line of control B, points I_2 and I_3 are the two intersection points of the region E and the line of control B (I_3 is farther away from I_1 than I_2), l_D is the length of the segment from I_1 to I_2, and l is the length of the segment from I_1 to I_3. Additionally, we consider a different case in our region-defense problem (see Fig. 1.(c)). The detailed proof of the directional derivatives can be found in [4]. Here we focus on the proof of the case in Fig. 1.(c).

Proof: 1) Perturbation along $\boldsymbol{\eta}_h$: As shown in Fig. 1(a), a perturbation ϵ along $\boldsymbol{\eta}_h$ changes the area of the intersection A by δA_h[2], where

$$\delta A_h = -\frac{l_D}{2} + O(\epsilon^2). \tag{13}$$

Therefore, the directional derivative of A along $\boldsymbol{\eta}_h$ is

$$D_hA = \lim_{\epsilon\to 0}\frac{\delta A_h}{\epsilon} = -\frac{l_D}{2}. \tag{14}$$

2) Perturbation along $\boldsymbol{\eta}_v$: We need to consider two different cases for a perturbation ϵ along $\boldsymbol{\eta}_v$. Fig. 1(b) shows the *first* case, where $\boldsymbol{\eta}_h$ intersects the region E. Such a perturbation ϵ causes A to change by $\delta A_v = \delta A_{v,2} - \delta A_{v,1}$. As the proof in [4], for the first case, we have

$$\delta A_v = \frac{(2ll_D - l_D^2)\epsilon}{2\,\|\boldsymbol{\xi}\|} + O(\epsilon^2). \tag{15}$$

Fig. 1(c) shows the *second* case, where $\boldsymbol{\eta}_h$ doesn't intersect the region E. Such a perturbation ϵ causes A to change by δA_v, where it is obvious that

$$\begin{aligned} \delta A_v &= \frac{(\frac{\epsilon}{2}+l)^2\tan\theta}{2} - \frac{(\frac{\epsilon}{2}+l-l_D)^2\tan\theta}{2} + O(\epsilon^2) \\ &= \frac{(\frac{\epsilon}{2}+l)^2\epsilon}{2\,\|\boldsymbol{\xi}\|} - \frac{(\frac{\epsilon}{2}+l-l_D)^2\epsilon}{2\,\|\boldsymbol{\xi}\|} + O(\epsilon^2) \\ &= \frac{\epsilon(\epsilon+2l-l_D)l_D}{2\,\|\boldsymbol{\xi}\|} + O(\epsilon^2). \end{aligned} \tag{16}$$

[2]In this letter we use $\delta A_{j,j=h,v}$ and $\delta L_{j,j=h,v}$ to represent the changes of A and L caused by the perturbations along $\boldsymbol{\eta}_h$ and $\boldsymbol{\eta}_v$, respectively.

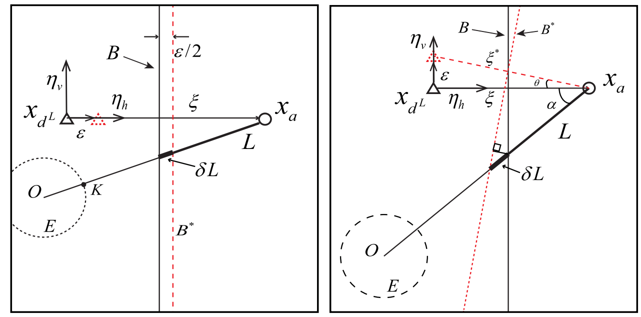

(a) (b)

Fig. 2. The variational changes of L with respect to (a) a perturbation along $\boldsymbol{\eta}_h$ and (b) a perturbation along $\boldsymbol{\eta}_v$.

Then, the directional derivative of A along $\boldsymbol{\eta}_v$ is

$$D_vA = \lim_{\epsilon\to 0}\frac{\delta A_v}{\epsilon} = \frac{2ll_D - l_D^2}{2\,\|\boldsymbol{\xi}\|}. \tag{17}$$

■

Finally, we can re-write the area-decreasing defense strategy $u_{d^A}^*$ (Eqn. (8)) for the defender d^A as

$$\begin{aligned} u_{d^A}^* \triangleq -(&\frac{\alpha_h^A}{\sqrt{|\alpha_h^A|^2+|\alpha_v^A|^2}}\cdot\boldsymbol{\eta}_h \\ &+\frac{\alpha_v^A}{\sqrt{|\alpha_h^A|^2+|\alpha_v^A|^2}}\cdot\boldsymbol{\eta}_v), \end{aligned} \tag{18}$$

where $\alpha_h^A = -l_D/2$ and $\alpha_v^A = (2ll_D - l_D^2)/(2\|\boldsymbol{\xi}\|)$.

Following a similar proof to that of the Lemma 1, we can derive the partial derivative $\partial A/\partial x_a$ as follows:

$$\frac{\partial A}{\partial x_a} = \alpha_h^A\boldsymbol{\eta}_h - \alpha_v^A\boldsymbol{\eta}_v. \tag{19}$$

B. Distance-Decreasing Defense Strategy

Now we consider the situation when A is empty. Let L be the distance between the attacker a and the intersection point of two lines, one of which is the line ao connecting x_a, the position of the attacker, and O, the center of the region E (see Fig. 2(a)), and the other is the line of control B. Point K is the intersection point of the line ao and the region E. We assign the defender that is closest to the point K as the *distance-decreasing defender* d^L with its position denoted by x_{d^L}. It is quite obviously that L is also the shortest distance between the attacker a and the region E inside the attacker's Voronoi cell V_a.

The role of distance-decreasing defender d^L is to minimize L. Since the time derivative of L is

$$\frac{\mathrm{d}L}{\mathrm{d}t} = \frac{\partial L}{\partial x_a}\dot{x}_a + \frac{\partial L}{\partial x_{d^L}}\dot{x}_{d^L}, \tag{20}$$

the strategy of d^L should be

$$u_{d^L}^* \triangleq -\frac{\partial L}{\partial x_{d^L}}\Big/\left\|\frac{\partial L}{\partial x_{d^L}}\right\|. \tag{21}$$

Similar to Section III-A, we can use vectors $\{\boldsymbol{\eta}_h, \boldsymbol{\eta}_v\}$ to define a local coordinate system based on x_a and x_{d^L}. For any $y \in \mathbb{R}^2$, define

$$L^*(y) = L(x_a, y + x_{d^L}, x_{d^1}, \ldots, x_{d^{N_D - 1}}). \tag{22}$$

Same as Eqn. (10), we can define $D_h L$ and $D_v L$ as the directional derivatives of L along $\boldsymbol{\eta_h}^D$ and $\boldsymbol{\eta_v}^D$, respectively. We then have the partial derivative of L with respect to x_{d^L} as follows:

$$\frac{\partial L}{\partial x_{d^L}} = D_h L \cdot \boldsymbol{\eta}_h + D_v L \cdot \boldsymbol{\eta}_v. \tag{23}$$

Lemma 2: For the distance-decreasing defender d^L, it is true that

$$D_h L = -\frac{L}{\|\boldsymbol{\xi}\|}, D_v L = \frac{L}{\|\boldsymbol{\xi}\|^2}\sqrt{4L_E^2 - \|\boldsymbol{\xi}\|^2}. \tag{24}$$

Proof: 1) Perturbation Along $\boldsymbol{\eta}_h$: As shown in Fig. 2(a), a perturbation ϵ along $\boldsymbol{\eta}_h$ moves the line of control B a distance of $\epsilon/2$ towards the position of the attacker x_a and changes the length L by δL_h. Due to the existence of similar triangles, we have

$$\frac{\delta L_h}{L} = \frac{\frac{\epsilon}{2}}{\frac{\|\boldsymbol{\xi}\|}{2}}. \tag{25}$$

Then we can get $\delta L_h = L\epsilon/\|\boldsymbol{\xi}\|$. Therefore the directional derivative of L along $\boldsymbol{\eta}_h$ can be derived as

$$D_h L = \lim_{\epsilon \to 0} \frac{\delta L_h}{\epsilon} = -\frac{L}{\|\boldsymbol{\xi}\|}. \tag{26}$$

2) *Perturbation along $\boldsymbol{\eta}_v$:* As shown in Fig. 2(b), when the defender d^L moves in the direction of $\boldsymbol{\eta}_v$ by a distance of ϵ, L will increase. Based on geometry, we can get

$$\delta L_v = \frac{(\frac{\epsilon}{2} + \sqrt{L^2 - \frac{\|\boldsymbol{\xi}\|^2}{4}})\sin\theta}{\cos(\theta + \alpha)}. \tag{27}$$

Then the directional derivative of L along $\boldsymbol{\eta}_v$ can be derived as

$$D_v L = \lim_{\epsilon \to 0} \frac{\delta L_v}{\epsilon} = \frac{L}{\|\boldsymbol{\xi}\|^2}\sqrt{4L_E^2 - \|\boldsymbol{\xi}\|^2}. \tag{28}$$

■

Finally, we can re-write the distance-decreasing defense strategy $u^*_{d^L}$ (Eqn. (21)) for the defender d^L as

$$\begin{aligned} u^*_{d^L} \triangleq -(&\frac{\alpha_h^L}{\sqrt{|\alpha_h^L|^2 + |\alpha_v^L|^2}} \cdot \boldsymbol{\eta}_h \\ &+ \frac{\alpha_v^L}{\sqrt{|\alpha_h^L|^2 + |\alpha_v^L|^2}} \cdot \boldsymbol{\eta}_v), \end{aligned} \tag{29}$$

where α_h^L and α_v^L are given by

$$\alpha_h^L = -\frac{L}{\|\boldsymbol{\xi}\|}, \alpha_v^L = \frac{L}{\|\boldsymbol{\xi}\|^2}\sqrt{4L_E^2 - \|\boldsymbol{\xi}\|^2}. \tag{30}$$

C. Overall Strategy and Proof of Guaranteed Capture

Our overall pursuit-defense strategy is summarized in Algo. (1). A defender is selected either as an area-decreasing defender d^A that follows the area-decreasing strategy $u^*_{d^A}$ (Eqn. (18)) or as a distance-decreasing defender d^L that follows the area-decreasing strategy $u^*_{d^L}$ (Eqn. (29)). All other defenders serve the role of pursuers and follow the "area-minimization strategy" proposed in [1] to capture the attacker a by moving towards the centroids of the shared Voronoi boundaries between the defenders and the attacker to minimize the attacker's Voronoi cell V_a.

Algorithm 1: Multi-Agent Pursuit-Defense Strategy.

```
Calculate all players's Voronoi cells using Eqn.s (5–6)
while min_{1≤i≤N}(‖x_{d^i} − x_a‖) > r_c do
  if any line of control B_i intersects E then
    Choose a defender as the area-decreasing defender
    d^A that implements u*_{d^A} (Eqn. (18))
  else
    Choose a defender as the distance-decreasing
    defender d^L that implements u*_{d^L} (Eqn. (29))
  end if
  Other defenders are pursuers and implement the
  "area-minimization strategy" proposed in [1]
  Re-calculate all players' Voronoi cells using Eqn.s
  (5–6)
end while
```

Lemma 3: For any admissible control input of the attacker a, under our area-decreasing defensive strategy $u^*_{d^A}$ (Eqn. (18)), $\mathrm{d}A/\mathrm{d}t \leq 0$. Moreover, $\mathrm{d}A/\mathrm{d}t = 0$ if and only if the strategy of the attacker is

$$\gamma^*(x_a, x_{d^A}) = \frac{\alpha_h^A \boldsymbol{\eta}_h - \alpha_v^A \boldsymbol{\eta}_v}{\sqrt{{\alpha_h^A}^2 + {\alpha_v^A}^2}}. \tag{31}$$

Proof: For an arbitrary d with $\|d\| \leq 1$:

$$\begin{aligned} \frac{\mathrm{d}A}{\mathrm{d}t} &= \frac{\partial A}{\partial x_{d^A}} u^*_{d^A} + \frac{\partial A}{\partial x_a} d \\ &= -\sqrt{{\alpha_h^A}^2 + {\alpha_v^A}^2} + (\alpha_h^A \boldsymbol{\eta}_h - \alpha_v^A \boldsymbol{\eta}_v)^T d \leq 0, \end{aligned} \tag{32}$$

where equality holds if and only if $d(t) = \gamma^*(x_a(t), x_{d^A}(t))$. ■

The squared Euclidean distance between the attacker a and the area-decreasing defender d^A is

$$z(x_a, x_{d^A}) = \|\xi(x_a, x_{d^A})\| = (x_a - x_{d^A})^T(x_a - x_{d^A}). \tag{33}$$

Lemma 4: Under our area-decreasing defence strategy $u^*_{d^A}$ (Eqn. (18)) and if $\dot{A} = 0$, $\mathrm{d}z(x_a, x_{d^A})/\mathrm{d}t < 0$.

Proof: From Lemma 3, we know that $\dot{A} = 0$ if and only if $d(t) = \gamma^*(x_a(t), x_{d^A}(t))$. Under our area-decreasing strategy $u^*_{d^A}$, we have (write $z(x_a, x_{d^A})$ as z)

$$\begin{aligned} \dot{z} &= 2(x_a - x_{d^A})^T(\dot{x_a} - \dot{x}_{d^A}) \\ &= 4\boldsymbol{\xi}^T \left(\frac{\alpha_h^A}{\sqrt{{\alpha_h^A}^2 + {\alpha_v^A}^2}} \boldsymbol{\eta}_h \right) \\ &= -\frac{4z}{\sqrt{z + (2l - l_D)^2}} < 0. \end{aligned} \tag{34}$$

when $\dot{A} = 0$. ■

Lemma 5: With respect to the local coordinate system (see Fig. 1(a)), the partial derivative $\partial L/\partial x_a$ under the distance-decreasing defense strategy $u^*_{d^L}$ (Eqn. (29)) is

$$\frac{\partial L}{\partial x_a} = \beta_h \boldsymbol{\eta}_h + \beta_v \boldsymbol{\eta}_v, \tag{35}$$

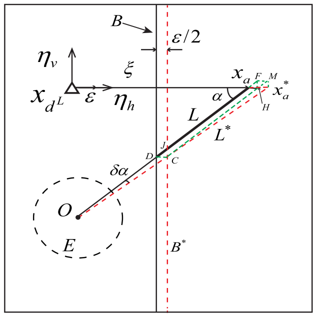

Fig. 3. This figure shows the geometric relationship involving the distance-decreasing defender d^L and the attacker a in the context of a perturbation along $\boldsymbol{\eta}_h$.

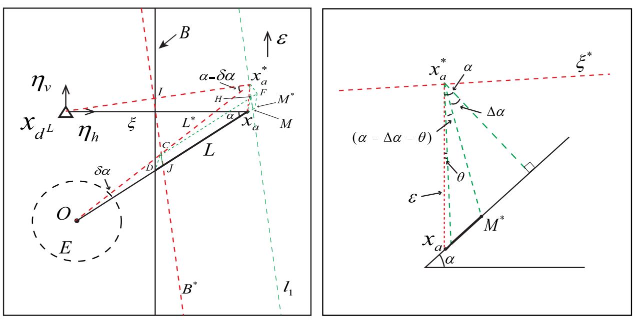

(a) (b)

Fig. 4. (a) shows the geometric relationship between the distance-decreasing defender d^L and the attacker a with respect to a perturbation along $\boldsymbol{\eta}_v$. (b) shows part of (a).

where $\beta_h = \cos\alpha/2$ and $\beta_v = \sin\alpha$ with α being the angle between the lines $x_a x_{d^L}$ and $x_a O$ (see Fig. 3).

Proof: 1) Perturbation along $\boldsymbol{\eta}_h$: As shown in Fig. 3, since $\triangle CDJ \cong \triangle F x_a H \cong \triangle HMF$, we have

$$\delta L_h = L^* - L = \frac{\epsilon}{2\cos\alpha} - \frac{\epsilon}{2}\tan\alpha\sin\alpha = \frac{\epsilon}{2}\cos\alpha. \quad (36)$$

Therefore, we can get

$$D_h L = \lim_{\epsilon\to 0}\frac{\delta L_h}{\epsilon} = \frac{\cos\alpha}{2} = \beta_h. \quad (37)$$

2) Perturbation along $\boldsymbol{\eta}_v$: Assume the attacker a moves in the direction of $\boldsymbol{\eta}_v$ by a distance of ϵ. From Fig. 4(a), we can observe that $\triangle CDJ \cong \triangle H x_a M$ and the total length of Dx_a and DJ is the same as that of DM. We can find a point M^* on DM such that $FM^* \parallel Hx_a$. Then we have

$$L^* - (L + DJ) = CF - DM = MM^* = JM^* - JM, \quad (38)$$

where $JM = L$ and

$$JM^* = \frac{Ix_a^*}{\cos\alpha - \theta} + (\epsilon\sin\alpha - \epsilon\cos\alpha\tan\delta\alpha), \quad (39)$$

Moreover, we have

$$\delta L_v = L^* - L. \quad (40)$$

Finally, similar to the way we calculated $D_h L$, we can get

$$D_v L = \lim_{\epsilon\to 0}\frac{\delta L_v}{\epsilon} = \sin\alpha - \cos\alpha\tan\delta\alpha = \sin\alpha = \beta_v. \quad (41)$$

■

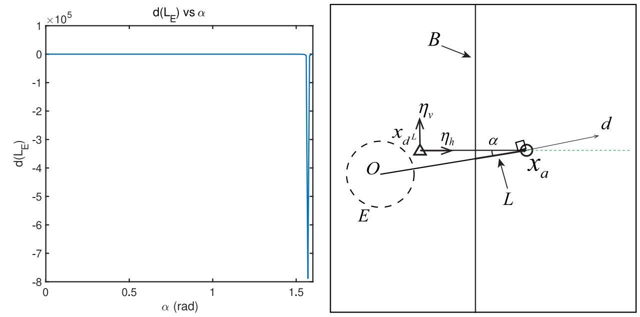

(a) (b)

Fig. 5. (a) shows $\mathrm{d}L/\mathrm{d}t$ over α. (b) shows that if the attacker a wants to satisfy $\mathrm{d}L/\mathrm{d}t > 0$, it can only move away from the region E.

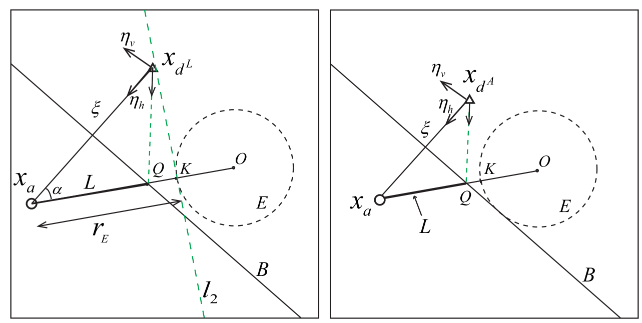

(a) (b)

Fig. 6. (a) shows that the distance-decreasing defender d^L can capture the attacker a outside the region E if there is no intersection. (b) shows the moment when an defender should switch to the area-decreasing strategy $u^*_{d^A}$.

Lemma 6: For any admissible attacker control input, as long as the attacker a moves towards the region E, $\mathrm{d}L/\mathrm{d}t < 0$ under our distance-decreasing strategy $u^*_{d^L}$ (Eqn. (29)).

Proof: For an arbitrary d with $\|d\| \le 1$, we have

$$\begin{aligned}\frac{\mathrm{d}L}{\mathrm{d}t} &= \frac{\partial L}{\partial x_{d^L}} u^*_{d^L} + \frac{\partial L}{\partial x_a} d \\ &= -\sqrt{{\alpha_h^L}^2 + {\alpha_v^L}^2} + (\beta_h \boldsymbol{\eta}_h + \beta_v \boldsymbol{\eta}_v)^T d.\end{aligned} \quad (42)$$

Assume $d \parallel \frac{\partial L}{\partial x_a}$ and $\|d\| = 1$. Then we can write $\mathrm{d}L/\mathrm{d}t$ as a function of α (see the definition of α in Lemma 3 and we have $0 < \alpha < \pi/2$) as follows:

$$\frac{\mathrm{d}L}{\mathrm{d}t} = \frac{1}{2\cos^2\alpha}\left(\sqrt{\cos^6\alpha + 4\sin^2\alpha\cos^4\alpha} - 1\right). \quad (43)$$

Fig. 5(a) shows how $\mathrm{d}L/\mathrm{d}t$ changes with respect to α according to Eqn. (43). We can see that when $\alpha > 0$, we have $\mathrm{d}L/\mathrm{d}t < 0$; when $\alpha = 0$, we have $\mathrm{d}L/\mathrm{d}t = 0$. In Fig. 5(b), we can see that, if $\alpha = 0$, the only way for the attacker a to keep $\mathrm{d}L/\mathrm{d}t = 0$ is to move along Ox_a. In this case, the attacker is moving away from the region E. ■

Theorem 1: (Guaranteed-Capture) From any initial configuration $\mathbf{x}_0 := ((x_a)_0, (x_{d^1})_0, \ldots, (x_{d^N})_0) \in D_d^*$ (Eqn. (4)), by following the strategy prescribed in Algo. (1), a group of defenders can always capture an attacker a outside the region E in a finite time, no matter what admissible strategy the attacker takes.

Proof: Under our strategy (Algo. (1)) and, as shown in Fig. 6(b), once the vertical bisector intersects the region E, a defender should be assigned as the area-decreasing defender d^A

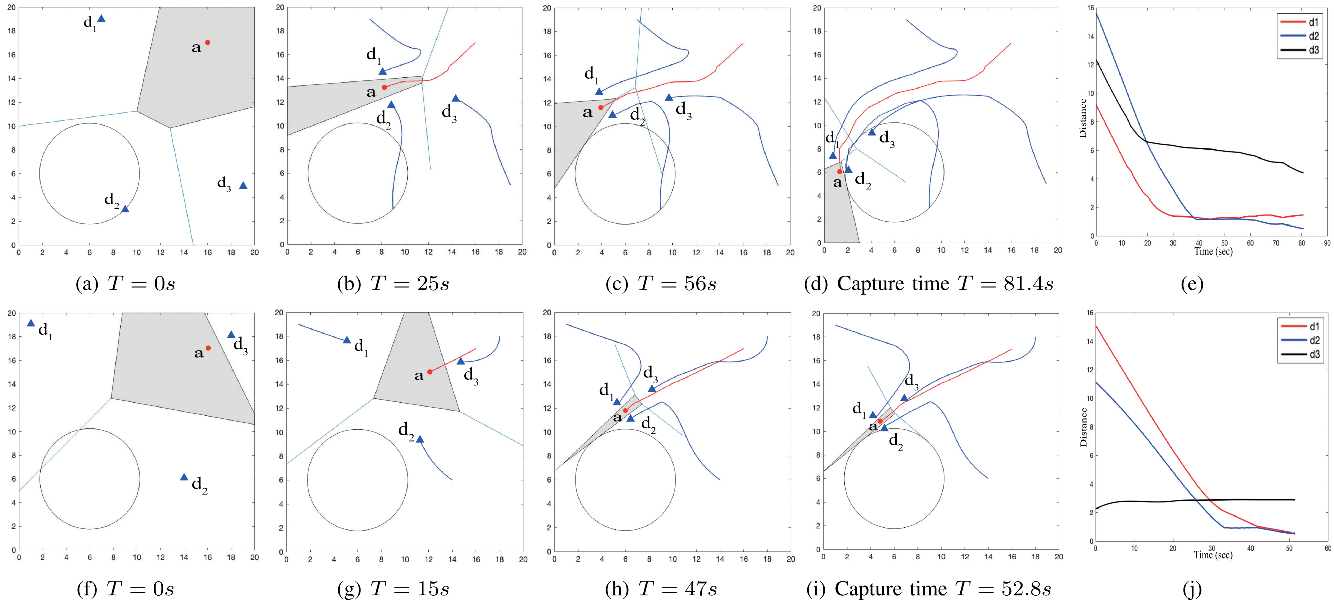

Fig. 7. (a)–(d) The game process of the three defenders and the single attacker a, where a's Voronoi cell is indicated by the grey shade. (e) The distances between a and the three defenders over time. (f)–(j) Simulation results of another game with different initial positions.

and switch to the area-decreasing strategy $u^*_{d^A}$. In the following, we will present our proof of guaranteed-capture based on whether there is such an intersection.

1) There is no intersection: As shown in Fig. 6(a), if the vertical bisector never intersects the region E, a defender is assigned to be the distance-decreasing defender d^L and takes the distance-decreasing strategy $u^*_{d^L}$ to decrease L and protect A (Lemma 6). At the same time, all the other defenders serve as pursuers and take the pursuing strategy described in [1] to decrease the safe-reachable area A of the attacker a. The capture of the attacker a in a finite time for this scenario has been proved in [1].

2) There is an intersection: Fig. 6(b) shows the moment when an intersection between the line of control B and the region E happens. Let's denote A by a positive δ. According to Algo. (1), at this moment, a defender is assigned to be the area-decreasing defender d^A and immediately switches to the area-decreasing strategy $u^*_{d^A}$. According to Lemma 3 and Lemma 4, we have:

- If the attacker a takes the strategy γ^* (Eqn. (31)), A will remain constant at δ and the line of control B will always be tangent to the region E. Therefore, $|QK| > 0$ will always be true. Moreover, according to Lemma 4, z (Eqn. (33)) will keep decreasing, resulting the distance-decreasing defender d^L to capture the attacker a outside the region E in a finite time.
- If the attacker a does not take the strategy γ^* (Eqn. (31)), we have$\mathrm{d}A/\mathrm{d}t < 0$. In this case, a defender will first assume the role of area-decreasing defender d^A to decrease A from ε to 0, then switch its strategy from $u^*_{d^A}$ to $u^*_{d^L}$, leading to the capture of a in a finite time.

■

IV. Simulation Results

To demonstrate the effectiveness of our strategy, we have tested its performance in a series of simulations where the attacker was controlled by humans, who tried to not only attack the region E but also evade the defenders when it was about to be captured. Fig. 7 shows the simulation results of three defenders (triangles) and one attacker (circle), in which the two rows represent two attack-defense games with different initial positions. The attack-defense game was played on a square region $D = [0, 20] \times [0, 20]$. The center of the region E was at (6,6) and the radius was $\sqrt{18}$. The defenders used the collaborative pursuit-defense strategy prescribed in Algo. (1). In Fig. 7(b), the defender d_2 is assigned to be the distance-decreasing defender d_L while the other two defenders are assigned to be the pursuers to decrease the attacker's Voronoi cell. In Fig. 7(c), the defender d_2 switches to take the area-decreasing strategy to defend the attacker from entering the region E. Fig. 7(d) shows the successful capture. Fig. 7(e) shows the distances between the attacker and the defenders over time. Consistent with *Theorem 1*, we can observe that although the attacker tries to enter the region E, the defender d_2 can always guarantee there is no intersection between the region E and the attacker's Voronoi cell V_a, which means there is always no chance for the attacker to enter the region E. From the game process shown in Fig. 7(a)–(d), a decreasing of the attacker's Voronoi cell V_a can be observed clearly. By comparing the two rows of Fig. 7, we can observe that the initial positions of the defenders affect the capture time.

While keeping all of the four agents in Fig. 7(a) at the same initial positions, we add one more defender d_4, as shown in Fig. 8. By comparing the simulation results shown in the first rows of Fig. 8 and Fig. 7, we can observe that, although the attacker takes a similar strategy, the capture happens sooner because the additional defender d_4 makes the attacker's Voronoi cell decrease faster. However, even when there is an additional defender, the attacker can still delay the capture by taking a different strategy, as shown in the second row of Fig. 8. By changing its strategy, the attacker can create a condition where two defenders d_1 and d_2 are left behind, which means these

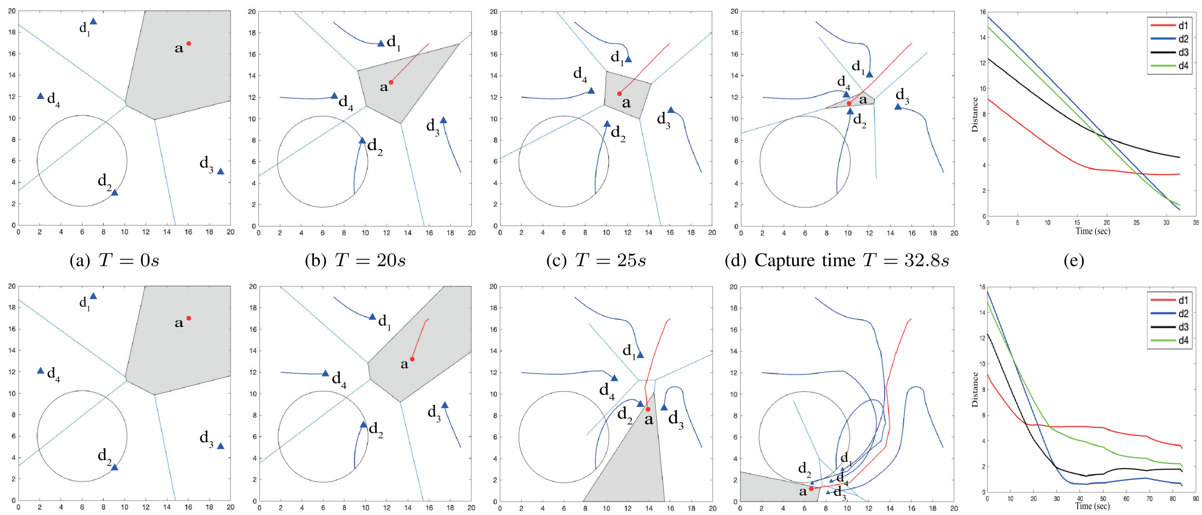

(a) $T = 0s$ (b) $T = 20s$ (c) $T = 25s$ (d) Capture time $T = 32.8s$ (e)

(f) $T = 0s$ (g) $T = 18s$ (h) $T = 40s$ (i) Capture time $T = 83.4s$ (j)

Fig. 8. Simulation results with five agents, where two rows represent different attack strategy. The meanings of the sub-figures are the same as Fig. 7.

two defenders will make no contribution to the decrease of the attacker's Voronoi cell (see Fig. 8(h)). Thus, we can observe that the capture time is related to the agents' initial positions and the attack strategy. Particularly, when the attacker is human-controlled, we can not make sure its strategy is aiming to enter region E at any time. Thus, although we can guarantee the capture, it is hard to get a specific capture time bound.

V. Conclusion

In this letter, we presented a collaborative pursuit-defense strategy to enable multiple defenders to defend a protected region from an attacker while attempting to capture the attacker outside the region. We have proven theoretically and demonstrated with simulations the guaranteed performance of our strategy. However, our work is based on the assumption of perfect information. In the future, we plan to expand our work to more realistic scenarios, for instance, with delayed communications and with obstacles and multiple attackers.

References

[1] A. Pierson, Z. Wang, and M. Schwager, "Intercepting rogue robots: An algorithm for capturing multiple evaders with multiple pursuers," *IEEE Robot. Autom. Lett.*, vol. 2, no. 2, pp. 530–537, Apr. 2017.

[2] H. Huang, W. Zhang, J. Ding, D. M. Stipanović, and C. J. Tomlin, "Guaranteed decentralized pursuit-evasion in the plane with multiple pursuers," in *Proc. 50th IEEE Conf. Decis. Control Eur. Control Conf.*, 2011, pp. 4835–4840.

[3] H. Huang, Z. Zhou, W. Zhang, J. Ding, D. M. Stipanovic, and C. J. Tomlin, "Safe-reachable area cooperative pursuit," *IEEE Trans. Robot.*, vol. 10, no. 5, pp. 10–15, Jul. 2012.

[4] Z. Zhou, W. Zhang, J. Ding, H. Huang, D. M. Stipanović, and C. J. Tomlin, "Cooperative pursuit with voronoi partitions," *Automatica*, vol. 72, pp. 64–72, 2016.

[5] Z. Zhou, R. Takei, H. Huang, and C. J. Tomlin, "A general, open-loop formulation for reach-avoid games," in *Proc. IEEE 51st IEEE Conf. Decis. Control*, 2012, pp. 6501–6506.

[6] M. Chen, Z. Zhou, and C. J. Tomlin, "A path defense approach to the multiplayer reach-avoid game," in *Proc. 53rd IEEE Conf. Decis. Control*, 2014, pp. 2420–2426.

[7] M. Chen, Z. Zhou, and C. J. Tomlin, "Multiplayer reach-avoid games via low dimensional solutions and maximum matching," in *Proc. Amer. Control Conf.*, 2014, pp. 1444–1449.

[8] M. Chen, Z. Zhou, and C. J. Tomlin, "Multiplayer reach-avoid games via pairwise outcomes," *IEEE Trans. Autom. Control*, vol. 62, no. 3, pp. 1451–1457, Mar. 2017.

[9] Z. Zhou, J. Ding, H. Huang, R. Takei, and C. Tomlin, "Efficient path planning algorithms in reach-avoid problems," *Automatica*, vol. 89, pp. 28–36, 2018.

[10] H. Huang, J. Ding, W. Zhang, and C. J. Tomlin, "Automation-assisted capture-the-flag: A differential game approach," *IEEE Trans. Control Syst. Technol.*, vol. 23, no. 3, pp. 1014–1028, May 2015.

[11] R. Isaacs, "A mathematical theory with applications to warfare and pursuit, control and optimization," New York, NY, USA: Wiley, 1965.

[12] H. Huang, J. Ding, W. Zhang, and C. J. Tomlin, "A differential game approach to planning in adversarial scenarios: A case study on capture-the-flag," in *Proc. IEEE Int. Conf. Robot. Autom.*, 2011, pp. 1451–1456.

[13] M. Ramana and M. Kothari, "A cooperative pursuit-evasion game of a high speed evader," in *Proc. 54th IEEE Conf. Decis. Control*, 2015, pp. 2969–2974.

[14] R. Takei, R. Tsai, Z. Zhou, and Y. Landa, "An efficient algorithm for a visibility-based surveillance-evasion game," *Commun. Math. Sciences*, Texas Univ., Austin, TX, USA, vol. 12, no. 7, pp. 1303–1327, 2014.

[15] S.-Y. Liu, Z. Zhou, C. Tomlin, and K. Hedrick, "Evasion as a team against a faster pursuer," in *Proc. Amer. Control Conf.*, 2013, pp. 5368–5373.

[16] S.-Y. Liu, Z. Zhou, C. Tomlin, and K. Hedri, "A gradient-based method for team evasion," in *Proc. ASME Dyn. Syst. Control Conf.*, 2013, pp. 1–9.

[17] S.-Y. Liu, Z. Zhou, C. Tomlin, and J. K. Hedrick, "Evasion of a team of dubins vehicles from a hidden pursuer," in *Proc. IEEE Int. Conf. Robot. Autom.*, 2014, pp. 6771–6776.

[18] J. F. Fisac and S. S. Sastry, "The pursuit-evasion-defense differential game in dynamic constrained environments," in *Proc. 54th IEEE Conf. Decis. Control*, 2015, pp. 4549–4556.

[19] M. Abdelkader, Y. Lu, H. Jaleel, and J. S. Shamma, "Distributed real time control of multiple UAVS in adversarial environment: Algorithm and flight testing results," in *Proc. IEEE Int. Conf. Robot. Autom.*, 2018, pp. 6659–6664.

[20] L. Liang, F. Deng, Z. Peng, X. Li, and W. Zha, "A differential game for cooperative target defense," *Automatica*, vol. 102, pp. 58–71, 2019.

[21] A. Ataei and I. C. Paschalidis, "Quadrotor deployment for emergency response in smart cities: A robust MPC approach," in *Proc. 54th IEEE Conf. Decis. Control*, 2015, pp. 5130–5135.

[22] A. Pierson, A. Ataei, I. C. Paschalidis, and M. Schwager, "Cooperative multi-quadrotor pursuit of an evader in an environment with no-fly zones," in *Proc. IEEE Int. Conf. Robot. Autom.*, 2016, pp. 320–326.